

Effect of induced magnetic field on natural convection in vertical concentric annuli

R. K. Singh · A. K. Singh

Received: 20 September 2010 / Revised: 21 March 2011 / Accepted: 16 June 2011

©The Chinese Society of Theoretical and Applied Mechanics and Springer-Verlag Berlin Heidelberg 2012

Abstract In the present paper, we have considered the steady fully developed laminar natural convective flow in open ended vertical concentric annuli in the presence of a radial magnetic field. The induced magnetic field produced by the motion of an electrically conducting fluid is taken into account. The transport equations concerned with the considered model are first recast in the non-dimensional form and then unified analytical solutions for the velocity, induced magnetic field and temperature field are obtained for the cases of isothermal and constant heat flux on the inner cylinder of concentric annuli. The effects of the various physical parameters appearing into the model are demonstrated through graphs and tables. It is found that the magnitude of maximum value of the fluid velocity as well as induced magnetic field is greater in the case of isothermal condition compared with the constant heat flux case when the gap between the cylinders is less or equal to 1.70 times the radius of inner cylinder, while reverse trend occurs when the gap between the cylinders is greater than 1.71 times the radius of inner cylinder. These fields are almost the same when the gap between the cylinders is equal to 1.71 times the radius of inner cylinder for both the cases. It is also found that as the Hartmann number increases, there is a flattening tendency for both the velocity and the induced magnetic field. The influence of the induced magnetic field is to increase the velocity profiles.

Keywords Natural convection · Isothermal · Heat flux · Skin-friction · Induced magnetic field · Magnetohydrodynamics

R. K. Singh
Department of Mathematics,
Central University of Bihar,
Patna, India

A. K. Singh (✉)
Department of Mathematics,
Banaras Hindu University,
Varanasi, India
e-mail: singhrajiv_78@rediffmail.com

Nomenclature

a	Radius of inner cylinder (m)
b	Radius of outer cylinder (m)
g	Acceleration due to gravity (m/s^2)
H'_z	Induced magnetic field in z' -direction (A/m)
H	Non-dimensional induced magnetic field in z -direction
J_θ	Induced current density (A/m^2)
M	Hartmann number
q'	Heat flux (W/m^2)
r', θ', z'	Cylindrical coordinates (m), ($^\circ$), (m)
r	Non-dimensional radial distance
T'_f	Ambient temperature (K)
T'_w	Temperature at outer surface of inner cylinder (at $r' = a$), (K)
T	Temperature of the fluid in non-dimensional form (K)
u	Fluid velocity in non-dimensional form along axial direction (m/s)
u'	Velocity of fluid along axial direction (m/s)
U	Characteristics velocity of fluid (m/s)

Greek symbols

β	Coefficient of thermal expansion
μ_e	Magnetic permeability (H/m)
η	Magnetic diffusivity
ϑ	Kinematic viscosity of the fluid (m^2/s)
ρ	Density of fluid (kg/m^3)
λ	Ratio of outer radius and inner radius, b/a
σ	Conductivity of fluid ($\text{A}^2\text{S}^{-3}/\text{kgm}^3$)

Subscript

1	Value at inner cylinder
λ	Value at outer cylinder
θ	Along θ -direction

1 Introduction

The annular geometry is widely employed in the analysis and design of heat exchangers. The study of transport phenomena in the context of annular geometry is gaining more attention from researchers because of its wide range of applications in the engineering as well as in the geophysics, such as the optimization of solidification processes of metals and metal alloys, the study of geothermal sources, the treatment of nuclear fuel debris, the control of underground spreading of chemical wastes and pollutants and the design of magnetohydrodynamic power generators. Ramamoorthy [1] has compared the classical hydrodynamic velocity with the magnetohydrodynamic velocity between two rotating co-axial cylinders in the presence of a radial magnetic field by neglecting the induced magnetic field. Later on, Arora and Gupta [2] have extended the same problem by taking into account the induced magnetic field.

Shaarawi and Sarhan [3] have studied the fully developed free convective flow in vertical annuli by considering isothermal heating or cooling of the inner cylinder and adiabatic condition on outer cylinder. Joshi [4] has investigated the fully developed free convective flow in vertical annuli with two isothermal boundaries. Further, Shaarawi and Nimb [5] have studied the effects of four fundamental boundary conditions by obtaining and comparing the corresponding fundamental solutions. These boundary conditions are obtained by combining each of the two conditions of having one boundary maintained at uniform heat flux or at uniform wall temperature with each of the conditions while the opposite boundary is kept isothermal at the inlet fluid temperature or adiabatic. Lee and Kuo [6] have discussed the laminar flow in annuli ducts imposed by constant wall temperature at the boundaries. Mahmud and Fraser [7] have focused on irreversibility characteristics in terms of entropy generation in fluid flow and heat transfer inside cylindrical annuli. Leong and Lai [8] have examined analytical solutions obtained through perturbation method and Fourier transform for the natural convection in concentric cylinders with a porous sleeve. Shaija and Narasimhan [9] have numerically investigated the coupled action of conduction, natural convection and surface radiation inside a horizontal annulus. Nada et al. [10] have investigated heat transfer characteristics of natural convective flow in the annulus between horizontal concentric cylinders using different types of nanofluids.

Jha [11] has analytically studied the natural convective flow along a vertical infinite plate under a constant magnetic field. Singh et al. [12] have studied the effect of mixed kind of thermal boundary conditions on the free convective flow of an electrically conducting fluid in annuli under the presence of a radial magnetic field. Several solutions in the case of hydromagnetic free-convective flows were obtained by Chandran et al. [13–16] and Singh et al. [17], by considering different physical situations of flow formation. Barletta et al. [18] have analyzed the combined forced and free flow of an electrically conducting fluid in vertical annular

porous medium surrounding a straight cylindrical electric cable. Singh and Singh [19] have presented solutions for mixed convective flow between two vertical walls.

The above studies on hydromagnetic free convective heat and mass transfer phenomena have been limited to the cases in which the induced magnetic field is neglected. This is because the mathematical descriptions as well as solution of such problems involve some less effort. The aim of the present paper is to perform a study of free convective flow of an electrically conducting fluid in vertical annular geometry in the presence of a radial magnetic field when the induced magnetic field is taken into account. Such type of field can be realized in the case of a motor or a loudspeaker. The unified solutions for the velocity, induced magnetic field, skin-friction and induced current density in non-dimensional form have been obtained using the mixed type of thermal conditions on the inner cylinder. Furthermore in order to resolve the singularity at $M = 2$, additional solutions have been given for this case. Finally, the influence of various parameters has been shown by graphs and tables.

2 Mathematical analysis

We have considered here steady laminar fully developed free convective flow of an electrically conducting fluid in the vertical concentric annulus of infinite length. The axis of the co-axial cylinders is taken as z' -axis and r' denotes the radial direction measured outward from the axis of cylinder. The radius of inner and outer cylinders is taken as a and b , respectively. Also the applied magnetic field is directed radially outward and is of the form aH'_0/r' . In the present physical situation the inner cylinder is heated or cooled either isothermally or at a constant heat flux so that its temperature (i.e. temperature of outer surface of the inner cylinder) is different from the ambient temperature T'_f . As the flow is fully developed and cylinders are of infinite length, the variables describing the flow formation depends only on the co-ordinate r' and as a result the velocity and magnetic fields are given by $[(0, 0, u'(r'))]$ and $[aH'_0/r', 0, H'_z(r')]$, respectively. Thus under the usual Boussinesq approximation, the basic transport equations [12, 20] for the considered model are obtained as follows

$$\vartheta \left(\frac{d^2 u'}{dr'^2} + \frac{1}{r'} \frac{du'}{dr'} \right) + g\beta (T' - T'_f) + \frac{a\mu_e H'_0}{\rho r'} \frac{dH'_z}{dr'} = 0, \quad (1)$$

$$\eta \left(\frac{d^2 H'_z}{dr'^2} + \frac{dH'_z}{dr'} \right) + \frac{aH'_0}{r'} \frac{du'}{dr'} = 0, \quad (2)$$

$$\frac{d^2 T'}{dr'^2} + \frac{1}{r'} \frac{dT'}{dr'} = 0. \quad (3)$$

The boundary conditions for the velocity, induced magnetic field and temperature field are

$$u' = H'_z = 0, \quad T' = T'_w \quad \text{or} \quad \frac{dT'}{dr'} = -q'/k, \quad \text{at} \quad r' = a, \quad (4)$$

$$u' = H'_z = 0, \quad T' = T'_f, \quad \text{at} \quad r' = b.$$

In the above equations, u' is the velocity of fluid, g is the acceleration due to gravity, μ is the coefficient of viscosity, μ_e is the magnetic permeability, T' is the temperature of fluid and β is the coefficient of volume expansion.

If we introduce the non-dimensional variables

$$u = u'/U, r = r'/a, \lambda = b/a, T = (T' - T'_\infty)/\Delta T, H = H'_z/a\sigma\mu_e H'_0 U, \tag{5}$$

where ΔT is $T'_w - T'_f$ or aq'/k according as inner cylinder is maintained at constant temperature T'_w or constant heat flux q' , the governing equations in the non-dimensional form are obtained as follows

$$\frac{d^2 u}{dr^2} + \frac{1}{r} \frac{du}{dr} + \frac{M^2}{r} \frac{dH}{dr} + T = 0, \tag{6}$$

$$\frac{d^2 H}{dr^2} + \frac{1}{r} \frac{dH}{dr} + \frac{1}{r} \frac{du}{dr} = 0, \tag{7}$$

$$\frac{d^2 T}{dr^2} + \frac{1}{r} \frac{dT}{dr} = 0. \tag{8}$$

The corresponding boundary conditions for the velocity, induced magnetic field and temperature field in dimensionless form are obtained as

$$u = H = 0, T = 1 \text{ or } \frac{dT}{dr} = -1, \text{ at } r = 1, \tag{9}$$

$$u = H = 0, T = 1, \text{ at } r = \lambda.$$

Additional non-dimensional physical parameters appearing in the above equations are the Hartmann number M and characteristic velocity U of the fluid defined by

$$M = \mu_e a H'_0 \sqrt{\sigma/\mu}, \tag{10}$$

$$U = g\beta a^2 \Delta T/\vartheta.$$

A unified solution for both the cases can be obtained by combining both conditions for the temperature field at the inner cylinder. By doing so, a combined condition is obtained as

$$A \frac{dT}{dr} + BT = C, \text{ at } r = 1, \tag{11}$$

in which by assigning suitable values to A , B and C the desired case can be obtained. The solutions of Eqs. (6)–(8) subject to their appropriate boundary conditions (9) and (11) are derived as follows

$$u = E_1 r^M + E_2 r^{-M} + E_3 + (D_2 \lg r + D_3) r^2, \tag{12}$$

$$H = E_4 + E_5 \lg r - (E_1 r^M - E_2 r^{-M})/M + [D_2(1 - 2 \lg r) - 2D_3] r^2/4, \tag{13}$$

$$T = \frac{C}{D_1} \lg(r/\lambda). \tag{14}$$

Using Eq. (12), the skin-frictions indimensionless form at outer surface of inner cylinder and inner surface of outer cylinder are given by

$$\tau_1 = \left(\frac{du}{dr}\right)_{r=1} = M(E_2 - E_1) + D_2 + 2D_3, \tag{15}$$

$$\tau_\lambda = -\left(\frac{du}{dr}\right)_{r=\lambda} = M(E_2 \lambda^{-(M+1)} - E_1 \lambda^{M-1}) - [D_2(1 + 2 \lg \lambda) + 2D_3] \lambda. \tag{16}$$

The induced current density along θ -direction obtained from the Maxwell's equation is given by

$$J_\theta = -\frac{dH}{dr} = -E_5 r^{-1} + E_1 r^{M-1} + E_2 r^{-(M+1)} + (D_2 \lg r + D_3) r. \tag{17}$$

Using the expression of the velocity and induced current density, the mass flux and induced current flux of the fluid through the annuli are obtained as

$$Q = 2\pi \int_1^\lambda r u dr = \pi \{ (\lambda^{M+2} - 1) E_1 / (M + 2) + (\lambda^{2-M} - 1) E_2 / (2 - M) + (\lambda^2 - 1) E_3 / 2 + [\lambda^4 (4 \lg \lambda - 1) + 1] D_2 / 16 + (\lambda^4 - 1) D_3 / 4 \}, \tag{18}$$

$$J = \int_1^\lambda J_\theta dr = -E_5 \lg \lambda + [E_1 (\lambda^M - 1) - E_2 (\lambda^{-M} - 1)] / M - (D_2 - 2D_3) (\lambda^2 - 1) / 4 + D_2 \lambda^2 \lg \lambda / 2. \tag{19}$$

Since the expressions (12) and (13) for the velocity and induced magnetic field contain the term $D_2 = 1/[2(4 - M^2)]$ and as a result of which we have to separately derive the solution for $M = 2.0$ in order to resolve the singularity. For $M = 2$, we have obtained expressions for the velocity and induced magnetic field separately and they are as follows

$$u = F_1 r^2 + F_2 r^{-2} + F_3 + (G_1 \lg r + G_2) r^2 \lg r, \tag{20}$$

$$H = F_2 r^{-2} / 2 + F_4 + F_5 \lg r + [G_9 + (G_{10} + G_{11} \lg r) \lg r] r^2. \tag{21}$$

By using the expression (20), the skin-friction at the cylindrical walls is obtained as

$$\tau_1 = 2(F_1 - F_2) + G_2, \tag{22}$$

$$\tau_\lambda = 2(F_1 \lambda - F_2 \lambda^{-3}) + 2(G_1 + G_2) \lambda \lg \lambda + 2G_1 \lambda (\lg \lambda)^2 + G_2 \lambda. \tag{23}$$

The induced current density along θ -direction is derived as

$$J_\theta = -[F_2 r^{-3} + F_5 r^{-1} + 2G_9 r + G_{10} r (2 \lg r + 1) + 2G_{11} r \lg r (\lg r + 1)]. \tag{24}$$

Further, the flux of fluid and induced current flux are obtained as follows

$$Q = 2\pi\left\{(\lambda^4 - 1)F_1/4 + \lg \lambda F_2 + (\lambda^2 - 1)F_3/2 + G_1\left[\lambda^4 \lg^2 \lambda - \lambda^4 \lg \lambda/2 + (\lambda^4 - 1)/8\right]/4 + G_2\left[\lambda^4(\lg \lambda - (\lambda^4 - 1)/4)/4\right]\right\}, \tag{25}$$

$$J = -\left\{(\lambda^{-2} - 1)F_2/2 + F_5 \lg \lambda + \left[G_9(\lambda^2 - 1) + (G_{10} + G_{11} \lg \lambda)\lambda^2 \lg \lambda\right]\right\}. \tag{26}$$

The constants $D_1, D_2, \dots, D_5; E_1, E_2, \dots, E_5; F_1, F_2, F_3$ and G_1, G_2, \dots, G_{11} appearing in the above equations are defined in the appendix.

3 Results and discussion

Singh et al. [12] have found that the temperature was higher in the case of isothermal condition than that in the constant heat flux case when the gap between the cylinders is less or equal to the radius of inner cylinder ($\lambda \leq 2$) while reverse phenomenon occurs when the gap is greater than the radius of inner cylinder ($\lambda > 2$). In light of these results, we concluded that there must exist a critical value of λ at which the temperature profiles will be the same for both the cases of thermal heating. Through numerical computations of Eq. (14), we have obtained that the temperature profiles are almost the same for both the cases of thermal heating when the critical value of $\lambda = 2.71$ (or gap ratio 1.71).

The outcomes from the numerical computations of analytical solutions are illustrated via figures and tables in order to analyze the behavior of the physical parameters on transport processes resulting from natural convection between coaxial cylinders. The velocities of the fluid for isothermal and constant heat flux cases are shown in Figs. 1, 2 and 3 for various values of the Hartmann number. It can be seen from Figs. 1 and 3 that the magnitude of maximum value of the velocity profile is higher in the case of isothermal condition than the case of constant heat flux when the radius of outer cylinder is less than 2.71 times the radius of inner cylinder ($\lambda < 2.71$) while reverse phenomena occur when $\lambda > 2.71$. Again, it is also clear from Fig. 2 that the velocity profiles for $\lambda = 2.71$ are approximately the same for both cases of thermal conditions imposed on the inner cylinder. This type of flow formation is expected as it arises from the temperature difference between the coaxial cylinders as explained earlier.

Further, the effect of Hartmann number is to decrease the velocity field for all range of λ (Figs. 1–3). We can also observe that the velocity profiles are becoming flatter in the middle region and sharper near the surface of the cylinder with increasing in value of the Hartmann number. For large values of Hartmann number, the fluid moves like a block, showing some sort of rigidity. It indicates that in the electrically conducting fluids strong magnetic field brings rigidity into the fluid flow.

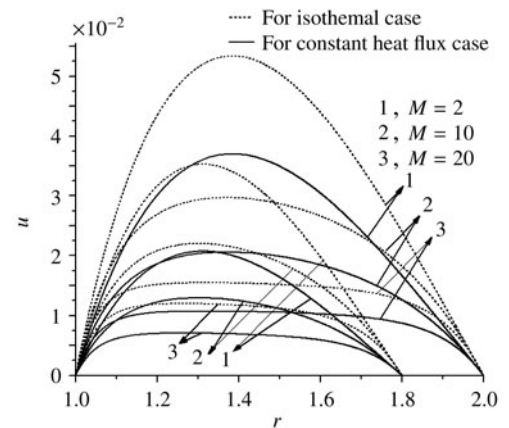


Fig. 1 Velocity profiles when $\lambda < 2.71$

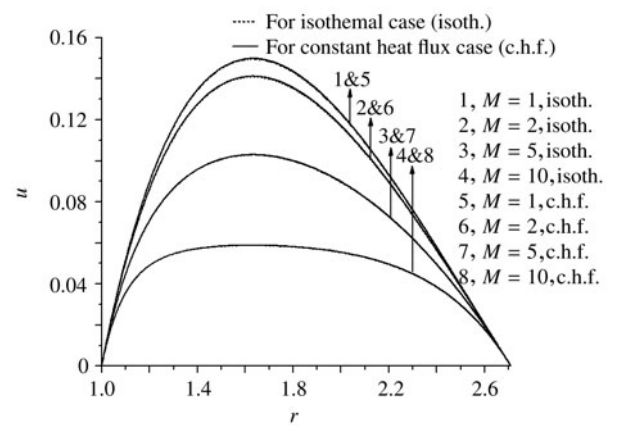


Fig. 2 Velocity profiles when $\lambda = 2.71$

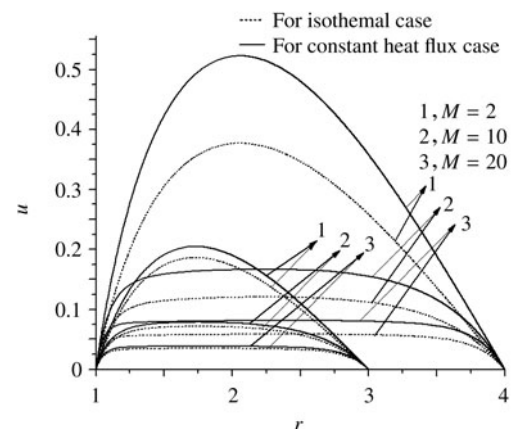


Fig. 3 Velocity profiles when $\lambda > 2.71$

In Figs. 4–6, we have shown the effect of magnetic field on the induced magnetic field for the cases when $\lambda \leftrightarrow 2.71$, respectively. We can see that in the region near the inner cylinder, the induced magnetic field is of parabolic type in upward direction and in the region near the outer cylinder, the induced magnetic field is also of

parabolic type but in opposite direction. A conclusive result from Figs. 4 and 6 is that when the gap between the cylinders is less than 1.71 times the radius on inner cylinder, the magnitude of induced magnetic field is large for the case of isothermal heating of the inner cylinder compared with the case of constant heat flux, while the situation is reversed when the gap between the cylinders

is greater than 1.71 times the radius of inner cylinder. Like the velocity field shown in Fig. 2, Fig. 5 also show that the induced magnetic field is the same for both types of thermal conditions when $\lambda = 2.71$.

We can also observe from these figures that the magnitude of maximum value of the induced magnetic field decreases as the Hartmann number increases and as a result the shape of the induced magnetic profile changes from parabolic to platykurtic type.

Figures 7–9 show the effect of Hartmann number on variation of the induced current density for three different values of λ ($= 2.0, 2.71$ and 4.0). It may be noted that the maximum value of positive induced current density occurs in the middle region of the flow. On the other hand, the maximum negative induced current density occurs on the surface of the cylinders. Further, we can observe that the effect of Hartmann number is to decrease both the positive induced current density in the middle region and the negative induced current density in the region near the cylinders. As expected, the effect of thermal boundary conditions on the induced current density depends on the gap between the cylinders just like the velocity and induced magnetic field. We can conclude from Figs. 7 and 9 that when the gap between the cylinders is less than 1.71 times the radius of inner cylinder, the magnitude of induced current density is higher for the case of isothermal heating on the inner cylinder than that in the case of constant heat flux, while the situation is reversed when the gap between the cylinders is greater than 1.71 times the radius of inner cylinder. Figure 8 shows that the induced current density is also the same as the velocity field for both thermal conditions when $\lambda = 2.71$. The magnitude of surface current density is greater on the inner cylinder compared to the outer cylinder for all the cases of fluid motion considered here.

In the Figs. 10–13, we have shown the effect of induced magnetic field by comparing the behavior of velocity profiles for both thermal conditions, (1) when the induced magnetic field is taken into account and (2) when the induced magnetic field is neglected [12].

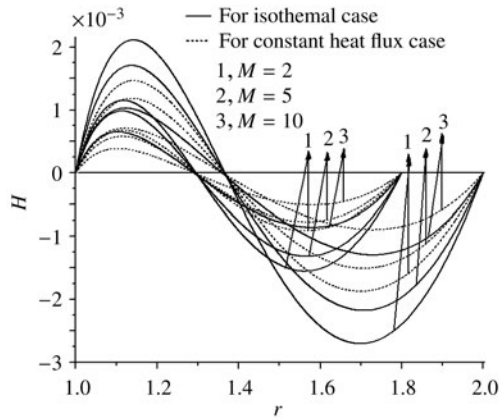


Fig. 4 Behavior of the induced magnetic field when $\lambda < 2.71$

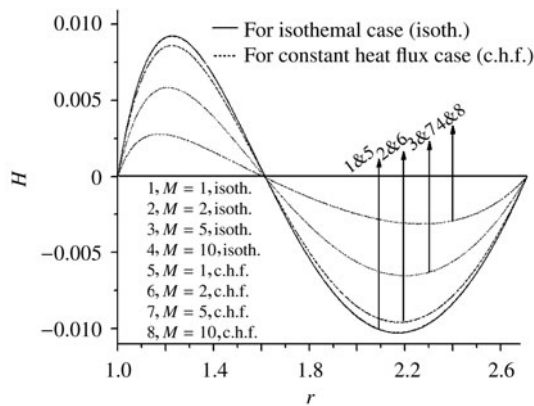


Fig. 5 Behavior of the induced magnetic field when $\lambda = 2.71$

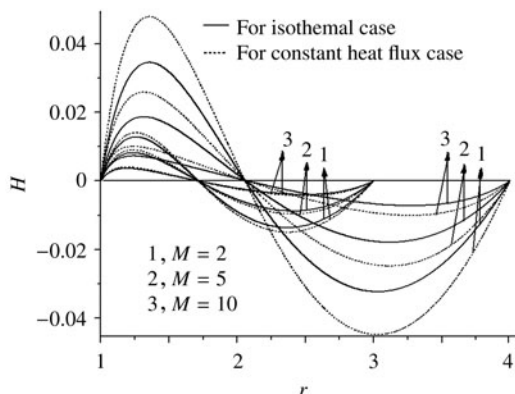


Fig. 6 Behavior of the induced magnetic field when $\lambda > 2.71$

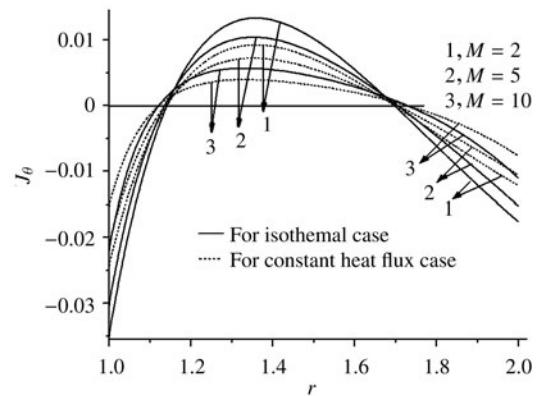


Fig. 7 Behavior of the induced current density when $\lambda = 2$

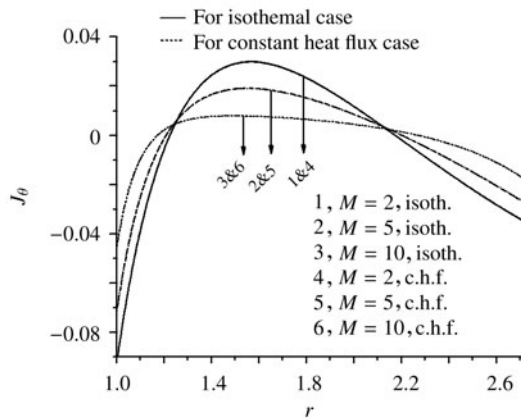


Fig. 8 Behavior of the induced current density when $\lambda = 2.71$

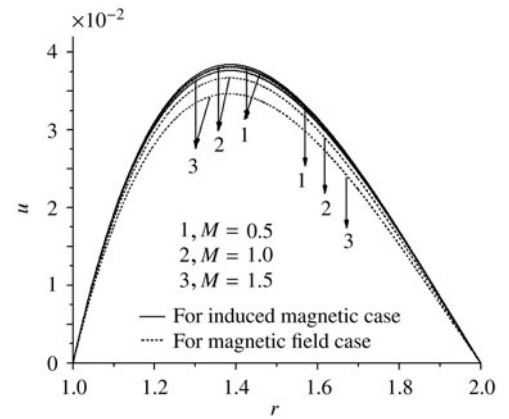


Fig. 11 Velocity profiles for the constant heat flux case when $\lambda = 2.0$

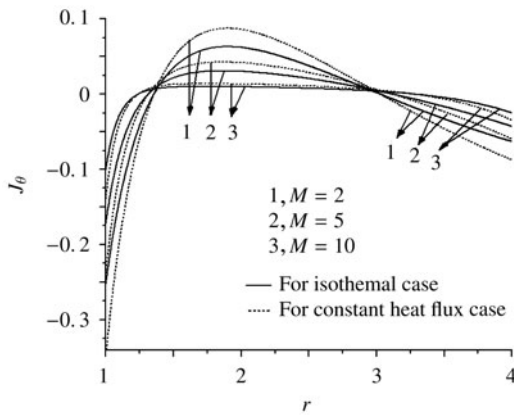


Fig. 9 Behavior of the induced current density when $\lambda = 4$

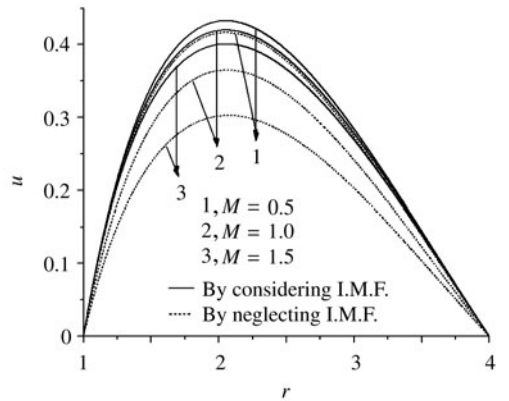


Fig. 12 Velocity profiles for the isothermal case when $\lambda = 4.0$

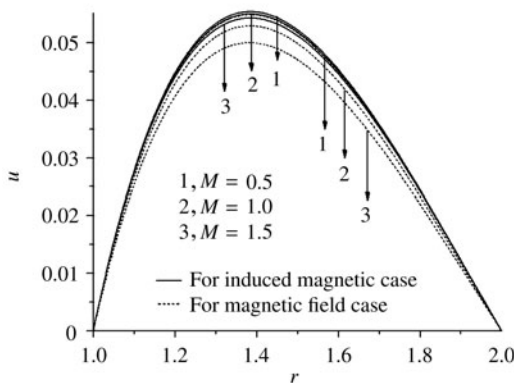


Fig. 10 Velocity profiles for the isothermal case when $\lambda = 2.0$

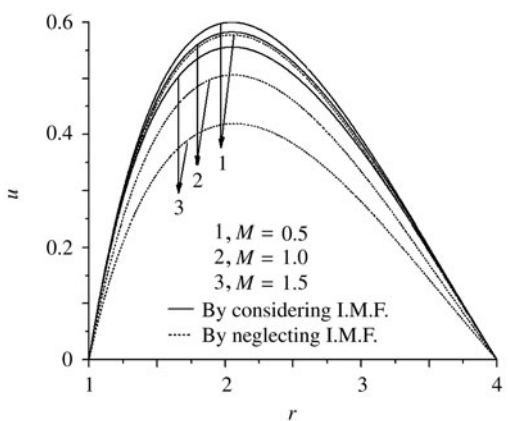


Fig. 13 Velocity profiles for the constant heat flux case when $\lambda = 4.0$

These figures show that for the same Hartmann number, the velocity profiles with considering the induced magnetic field taken into account are increased compared to the case of neglecting the induced magnetic field for both types of thermal boundary conditions.

The numerical values of skin-friction τ_1 (at the outer surface of inner cylinder) and τ_2 (at the inner surface of outer cylinder) are given in Table 1. From this table, we can observe clearly that the ratio of radii of outer to inner cylinders

has great impact upon the skin-friction. From the comparative study of the numerical values of skin-friction for the cases of isothermal and constant heat flux, we can conclude that when the gap between cylinders is less or equal to 1.71 times the radius of inner cylinder ($\lambda = 2.71$, then τ_1 and τ_λ are more for isothermal heating of the inner cylinder than those in the constant heat flux case while the situation is reversed when the gap between cylinders is greater than 1.71

times the radius of inner cylinder. Further, the influence of increasing the gap between inner and outer cylinder (λ) on τ_1 and τ_λ is to increase them. The applied magnetic field has a tendency to decrease the skin-friction at outer surface of the inner cylinder while to increase the skin-friction at inner surface of the outer cylinder when $\lambda < 4$ and the behavior of skin-friction is reversed for $\lambda = 4$.

Table 1 Numerical values of skin-friction for isothermal and constant heat flux cases

λ	M	τ_1	τ_1	τ_λ	τ_λ
		(Iso. temp.)	(C. h. f.)	(Iso. temp.)	(C. h. f.)
1.8	0.5	0.270 16	0.158 80	0.101 42	0.059 62
	1.0	0.269 98	0.158 69	0.101 52	0.059 67
	1.5	0.269 69	0.158 52	0.101 69	0.059 77
	2.0	0.269 29	0.158 29	0.101 91	0.059 90
2.0	0.5	0.339 59	0.235 39	0.121 22	0.084 02
	1.0	0.339 32	0.235 20	0.121 35	0.084 11
	1.5	0.338 89	0.234 90	0.121 56	0.084 26
	2.0	0.338 31	0.234 50	0.121 86	0.084 47
3.0	0.5	0.701 85	0.771 06	0.206 21	0.226 55
	1.0	0.701 54	0.770 72	0.206 31	0.226 66
	1.5	0.701 04	0.770 18	0.206 48	0.226 84
	2.0	0.700 40	0.769 47	0.206 69	0.227 08
4.0	0.5	1.091 11	1.512 60	0.278 49	0.386 06
	1.0	1.092 54	1.514 58	0.278 13	0.385 57
	1.5	1.094 70	1.517 57	0.277 59	0.384 82
	2.0	1.097 32	1.521 21	0.276 93	0.383 91

The numerical values of Q (mass flow rate) and induced current flux through the annulus region for both types of ther-

mal conditions at the outer surface of the inner cylinder are given in Table 2.

Table 2 Numerical values of fluid flux and induced current flux for isothermal and constant heat flux cases

λ	M	Q	Q	$J/10^{-16}$	$J/10^{-16}$
		(Iso. temp.)	(C.h.f.)	(Iso. temp.)	(C.h.f.)
1.8	0.5	0.159 43	0.093 71	8.82	-1.11
	1.0	0.158 74	0.093 31	2.22	1.66
	1.5	0.157 61	0.092 64	-13.2	-4.44
	2.0	0.156 10	0.091 74	-0.208	0
2.0	0.5	0.323 75	0.224 41	1.11	-4.41
	1.0	0.321 81	0.223 06	-2.22	4.99
	1.5	0.318 65	0.220 87	15.5	7.77
	2.0	0.314 37	0.217 90	-27.7	0.116
3.0	0.5	3.075 01	3.378 25	-4.41	-15.5
	1.0	3.029 72	3.328 49	-2.22	-2.22
	1.5	2.958 30	3.250 03	-17.7	17.7

Table 2 Numerical values of fluid flux and induced current flux for isothermal and constant heat flux cases (continued)

λ	M	Q		$J/10^{-16}$	
		(Iso. temp.)	(C.h.f.)	(Iso. temp.)	(C.h.f.)
4.0	2.0	2.865 98	3.148 60	0.555	0
	0.5	11.960 7	16.581 1	13.3	0
	1.0	11.686 8	16.201 3	0	4.44
	1.5	11.267 9	15.620 6	8.88	26.6
	2.0	10.748 4	14.900 5	-3.33	-2.22

As expected, the Hartmann number always tends to reduce the mass flux of fluid Q for both types of thermal conditions. The increase in the values of Hartmann number yields oscillatory nature in the induced current flux with decreasing amplitude while the amplitude of induced current flux increase enhances with increasing gap between the cylinders for both types of thermal conditions on the inner cylinder. It can also be observed that the fluid flux is larger in the case of isothermal condition than that in the constant heat flux case $\lambda < 2.71$ while the reverse phenomenon occurs when $\lambda > 2.71$.

4 Conclusions

We have theoretically investigated the effects of radii ratio parameter and Hartmann number, on the free convective flow of an electrically conducting fluid generated by imposing mixed type of thermal conditions on the surface of inner cylinder in the presence of a radial magnetic field with the induced magnetic field taken into account. It is found that Hartmann number and the gap between cylinders play important roles in controlling the behavior of fluid flow. By a comparative study, it is observed that the effect of the induced magnetic field is to increase the velocity profiles. As the Hartmann number increases, the magnitude of maximum value of the velocity has a decreasing tendency, and the velocity tends to take a uniform value in the middle region for higher values of Hartmann number. This flattening tendency is also observed in the induced magnetic field and induced current density. The magnitude of surface current density is greater on the inner cylinder compared to the outer cylinder. In general, skin-friction, mass flux of fluid and induced current density can be increased by increasing the gap between the cylinders. The effect of magnetic field on the skin-friction can be useful in mechanical engineering for modeling a system. We can easily obtain a suitable value of Hartmann number for which the value of the skin-friction will be optimum.

Appendix

$$D_1 = A - B \lg \lambda, \quad D_2 = -C/[D_1(4 - M^2)],$$

$$D_3 = C \left[(12 - M^2)/(4 - M^2) + 2 \lg \lambda - 1 \right] / [2D_1(4 - M^2)],$$

$$D_4 = \left\{ (\lambda^2 - 1)[D_2 + 2D_3 - C/(4D_1)] + 2 \lg \lambda [\lambda^2 D_2 + C/(4D_1)] \right\} / M,$$

$$D_5 = D_2 \lambda^2 \lg \lambda + D_3(\lambda^2 - 1),$$

$$E_1 = (D_4 + D_5)/[2(1 - \lambda^M)],$$

$$E_2 = (-D_4 + D_5)/[2(1 - \lambda^{-M})],$$

$$E_3 = -E_1 - E_2 - D_3,$$

$$E_4 = (E_1 - E_2)/M - (D_2 - 2D_3)/4,$$

$$E_5 = \left\{ (E_1 \lambda^M - E_2 \lambda^{-M})/M + \lambda^2 [D_2(2 \lg \lambda - 1) + 2D_3]/4 - E_4 \right\} / \lg \lambda,$$

$$G_1 = -C/(8D_1), \quad G_2 = C(1 + 4 \lg \lambda)/(16D_1),$$

$$G_3 = -\lambda^2 \lg \lambda (G_1 \lg \lambda + G_2),$$

$$G_4 = -[2G_1 + G_2 + C/(4D_1)],$$

$$G_5 = -(2G_1 + 4G_2 - C \lg \lambda / D_1)/4,$$

$$G_6 = (G_1 + G_4)/2, \quad G_7 = [2G_5 - (G_1 + G_4)]/4,$$

$$G_8 = -\lambda^2 \lg \lambda (G_1 \lg \lambda - 2G_6) + 2G_7(\lambda^2 - 1),$$

$$G_9 = -(2F_1 + G_1 - G_2)/4, \quad G_{10} = (G_1 - G_2)/2,$$

$$G_{11} = -G_1/2,$$

$$F_1 = (G_3 + G_8)/[2(\lambda^2 - 1)],$$

$$F_2 = (G_3 - G_8)/[2(\lambda^{-2} - 1)],$$

$$F_3 = -(F_1 + F_2), \quad F_4 = -(G_9 + F_2/2),$$

$$F_5 = -\left[F_4 + G_9 \lambda^2 + (G_{10} + G_{11} \lg \lambda) \lambda^2 \lg \lambda + F_2/(2\lambda^2) \right] / \lg \lambda.$$

References

- 1 Ramamoorthy, P.: Flow between two concentric rotating cylinders with a radial magnetic field. *The Physics of Fluids* **4**, 1444–1445 (1961)
- 2 Arora, K. L., Gupta, P. R.: Magnetohydrodynamic flow between two rotating coaxial cylinders under radial magnetic field. *The Physics of Fluid* **15**, 1146–1148 (1971)
- 3 El-Shaarawi, M. A. I., Sarhan, A.: Developing laminar free convection in an open ended vertical annulus with a rotating inner cylinder. *Journal of Heat Transfer* **103**, 552–558 (1981)
- 4 Joshi, H. M.: Fully developed natural convection in an isothermal vertical annular duct. *International Communications in Heat and Mass Transfer* **14**, 657–664 (1987)

- 5 El-Shaarawi, M. A. I., Al-Nimb, M. A.: Fully developed laminar natural convection in open ended vertical concentric annuli. *International Journal of Heat and Mass Transfer* **33**, 1873–1884 (1990)
- 6 Lee, Y. M., Kuo, Y. M.: Laminar flow in annuli ducts with constant wall temperature. *International Communications in Heat and Mass Transfer* **25**, 227–236 (1998)
- 7 Mahmud, S., Fraser, R. A.: Irreversibility analysis of concentrically rotating annuli. *International Communications in Heat and Mass Transfer* **29**, 697–706 (2002)
- 8 Leong, J. C., Lai, F. C.: Natural convection in concentric annulus with a porous sleeve. *International Journal of Heat and Mass Transfer* **49**, 3016–3027 (2006)
- 9 Shaija, A., Narasimham, G. S. V. L.: Effect of surface radiation on conjugate normal convection in a horizontal annulus driven by inner heat generating solid cylinder. *International Journal of Heat and Mass Transfer* **52**, 5759–5769 (2009)
- 10 Abu-Nada, E., Masoud, Z., Hijazi, A.: Natural convection heat transfer enhancement in horizontal concentric annuli using nanofluids. *International Communications in Heat and Mass Transfer* **35**, 657–665 (2008)
- 11 Jha, B. K.: MHD free-convection and mass transform through a porous media. *Astrophysics and Space Science* **175**, 283–289 (1990)
- 12 Singh, S. K., Jha, B. K., Singh, A. K.: Natural convection in vertical concentric annuli under a radial magnetic field. *Heat and Mass Transfer* **32**, 399–401 (1997)
- 13 Chandran, P., Sacheti, N. C., Singh, A. K.: Effects of rotation on unsteady hydrodynamic Couette flow. *Astrophysics and Space Science* **202**, 1–10 (1993)
- 14 Chandran, P., Sacheti, N. C., Singh, A. K.: Singh, Haydro-magnetic flow and heat transfer past a continuously moving porous boundary. *International Communications in Heat and Mass Transfer* **23**, 889–898 (1996)
- 15 Chandran, P., Sacheti, N. C., Singh, A. K.: Unsteady hydro-magnetic free convection flow with heat flux and accelerated boundary motion. *Journal of Physical Society of Japan* **67**, 124–129 (1998)
- 16 Chandran, P., Sacheti, N. C., Singh, A. K.: A unified approach to analytical solution of a hydromagnetic free convection flow. *Scientiae Mathematicae Japonicae* **53**, 467–476 (2001)
- 17 Singh A. K. Chandran, P. Sacheti, N. C.: Effects of transverse magnetic field on a flat plate thermometer problem. *International Journal of Heat and Mass Transfer* **43**, 3253–3258 (2000)
- 18 Barletta, A., Lazzari, A., Magyari, E., et al.: Mixed convection with heating effects in a vertical porous annulus with a radially varying magnetic field. *International Journal of Heat and Mass Transfer* **51**, 5777–5784 (2008)
- 19 Singh, R. K., Singh, A. K.: Hydromagnetic mixed convection between two vertical walls. *Journal of Energy, Heat and Mass Transfer* **31**, 111–123 (2009)
- 20 Chandrasekhar, S.: *Hydrodynamic and Hydromagnetic Stability*, Oxford, England (1961)